Polarizability of conducting sphere-doublets using series of images

Henrik Wallén[a)] and Ari Sihvola

Electromagnetics Laboratory, Helsinki University of Technology, P.O. Box 3000 FIN-02015 HUT, Finland

The classical electrostatic problem of two nonintersecting conducting spheres in a uniform incident electric field is considered. Starting from the basic Kelvin's image principle, the two spheres are replaced with equivalent series of image sources, from which the polarizability is calculated. Explicit expressions for the axial and transversal components of the polarizability dyadic are found by solving the recurrence equations. Efficient numerical evaluation of the different series is also discussed. © *2004 American Institute of Physics.* [DOI: 10.1063/1.1769094]

I. INTRODUCTION

Polarizability is one of the basic parameters describing the electrostatic response of a given object. It is of great importance in modeling of the effective permittivity of random and ordered heterogeneous materials as well as the first-order scattering effects. Accurate information of the polarizability of interacting objects helps us to find a more realistic model for a dense material mixture where scatterers are closely located to each other.

In this paper we consider the electrostatic boundary problem of two conducting spheres of radius a, distance L apart as shown in Fig. 1, placed in a uniform incident electric field $\mathbf{E}_0$. We restrict the consideration to the nonintersecting case, $L > 2a$, and only consider the polarizability of the doublet.

The problem is not new and numerous solutions and applications have been presented, but there is still room for improvement for the solution of this canonical problem.

Perhaps the first complete solution, based on solving the Laplace's equation in bispherical, coordinates, was presented by Levine and McQuarrie.[1] Solutions using series of images have also been presented, e.g., in Refs. 2–4. However, all presented results contain infinite series, in one form or another. The limiting case of touching spheres has an analytic solution. All series converge rapidly when the distance between the spheres is large, but near contact the convergence is very slow.

The intersecting case, $L < 2a$, has also been considered in many papers. Recently, Felderhof and Palaniappan[5] presented a general solution in integral form. The integrals can easily be numerically evaluated with high accuracy, so therefore we can consider the intersecting case solved.

II. POLARIZABILITY

The polarizability of an object is a measure of its response to an incident electric field. Assume a uniform electric field $\mathbf{E}_0$ in a homogeneous space with permittivity ϵ. When we introduce an object in the incident field, the total field will be perturbed. If the object has no net charge, it can be approximated by its induced dipole moment $\mathbf{p}$, and the

polarizability is defined as the ratio between the induced dipole moment $\mathbf{p}$ and the amplitude of the incident field $\mathbf{E}_0$.

In general, the polarizability is a linear mapping that can be expressed using a dyadic $\bar{\bar{\alpha}}$ as

$$\mathbf{p} = \bar{\bar{\alpha}} \cdot \mathbf{E}_0. \tag{1}$$

Let us define the normalized polarizability of an object as

$$\bar{\bar{\alpha}}_n = \frac{\bar{\bar{\alpha}}}{\epsilon V}, \tag{2}$$

where ϵ is the permittivity of the surrounding space and V is the volume of the object. With this definition the normalized polarizability of a conducting object depends only on the shape of the object.

Consider first one conducting sphere of radius a in a uniform incident field $\mathbf{E}_0$. The perturbation of the field outside the sphere can be calculated exactly by replacing the sphere with a dipole

$$\mathbf{p} = 3\epsilon V \mathbf{E}_0 = 4\pi\epsilon a^3 \mathbf{E}_0 \tag{3}$$

at the center of the sphere.[6] Thus, the normalized polarizability of a conducting sphere is a scalar $\alpha_n = 3$.

Consider now the polarizability of the conducting sphere doublet in Fig. 1. Due to the rotational symmetry, the polarizability dyadic must be axial. Choosing the coordinate system such that the symmetry axis is parallel to the z axis, we can express the normalized polarizability as

$$\bar{\bar{\alpha}}_n = \alpha_t(\mathbf{u}_x\mathbf{u}_x + \mathbf{u}_y\mathbf{u}_y) + \alpha_z\mathbf{u}_z\mathbf{u}_z, \tag{4}$$

where α_t and α_z are the normalized transversal and axial polarizabilities.

III. KELVIN'S IMAGE PRINCIPLE

The Kelvin's image principle[7] offers an elegant solution for the electrostatic boundary problem of a point charge near a conducting sphere. Consider a point charge Q at distance
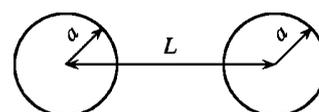

FIG. 1. Geometry of the problem: a pair of conducting spheres.

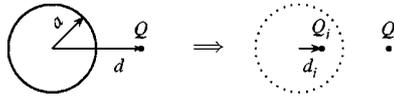[a)]Electronic mail: henrik.wallen@hut.fi

FIG. 2. Kelvin's image principle for a point charge near a grounded conducting sphere.

$d > a$ from the center of a grounded conducting sphere with radius a as in Fig. 2. The potential outside the sphere remains the same if we replace the sphere with an image point charge

$$Q_i = -\frac{a}{d}Q, \tag{5}$$

inside the sphere at the inverse point

$$d_i = \frac{a^2}{d}. \tag{6}$$

If the sphere is insulated we need to add a balancing charge $-Q_i$ at the center of the sphere to get zero total charge on the sphere.

The image principle for a dipole can be obtained by considering a system of two point charges $+Q$ and $-Q$ separated by a distance b. Letting $b \rightarrow 0$, while keeping the dipole moment $p = Qb$ constant, we get the image systems shown in Fig. 3. In the transversal case, we get an oppositely directed image dipole

$$\mathbf{p}_i = -\frac{a^3}{d^3}\mathbf{p} \tag{7}$$

at the inverse point d_i. In the radial case, we get a dipole $\mathbf{p}_i$ as well as a point charge Q_i at the inverse point d_i:

$$\mathbf{p}_i = \frac{a^3}{d^3}\mathbf{p}, \quad Q_i = \pm\frac{a}{d^2}|\mathbf{p}| \tag{8}$$

where $Q_i > 0$ if the dipole $\mathbf{p}$ is directed away from the sphere as in the figure and $Q_i < 0$ in the opposite case. For an insulated sphere we also need to add a charge $-Q_i$ at the center of the sphere to get a zero total charge.

A system of two nonintersecting conducting spheres can be replaced by infinite series of images inside both spheres. This idea is about as old as the basic Kelvin's image principle itself,[8] and it has also been treated in several books, e.g., by Maxwell[9] and Smythe[10] for calculating the capacitance of two spheres.
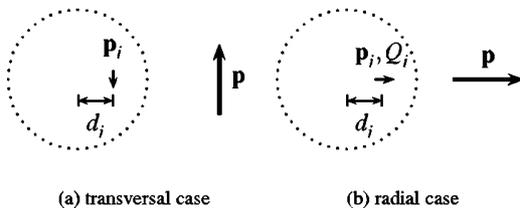

(a) transversal case   (b) radial case

FIG. 3. Images for a dipole $\mathbf{p}$ at distance d from the center of a conducting sphere of radius a.
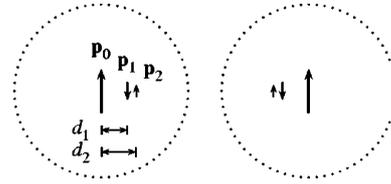

FIG. 4. Image systems for the transversal case.

IV. IMAGE SYSTEMS FOR THE SPHERE DOUBLET

To solve the polarizability of the sphere doublet, it is sufficient to consider the cases of transversal and axial excitations ($\mathbf{E}_0 \perp \mathbf{u}_z$ and $\mathbf{E}_0 \| \mathbf{u}_z$, respectively).

In both cases we replace the spheres by equivalent image sources. To solve the polarizability components we need to compute the total induced dipole moment, which we get by summing the dipole moments of the image dipoles and pairs of image point charges.

A. Transversal case

In the transversal case the excitation $\mathbf{E}_0$ is perpendicular to the symmetry axis of the doublet. In this case the image series will just consist of dipoles $\mathbf{p}_n \| \mathbf{E}_0$.

To construct the image series we proceed as follows: First replace each sphere with a dipole $\mathbf{p}_0 = 3\epsilon V \mathbf{E}_0$ at the center of the sphere. Then add dipoles $\mathbf{p}_1$ using Eq. (7) to compensate for the first dipoles. Further, add dipoles $\mathbf{p}_2$ to compensate for the dipoles $\mathbf{p}_1$ and so on as shown in Fig. 4.

We can express the image positions as distances from the center of the spheres as

$$d_0 = 0, \quad d_{n+1} = \frac{a^2}{L - d_n}, \tag{9}$$

and the amplitudes of the dipoles are

$$p_0 = 3\epsilon V E_0, \quad p_{n+1} = \frac{a^3}{(L - d_n)^3}p_n. \tag{10}$$

The induced dipole moment is simply the sum of all dipoles $\mathbf{p}_n$. Thus, the normalized polarizability is

$$\alpha_t = \frac{1}{\epsilon V E_0}\sum_{n=0}^{\infty}(-1)^n p_n = 3\sum_{n=0}^{\infty}(-1)^n\frac{p_n}{p_0}. \tag{11}$$

Since the dipoles have alternating directions, we get an alternating sum for the normalized polarizability.

In the touching limit, when $L \rightarrow 2a$, the solutions of Eqs. (9) and (10) are

$$d_n = \frac{n}{n+1}a, \quad p_n = \frac{p_0}{(n+1)^3}, \tag{12}$$

as is easy to verify. The limiting value for the normalized transversal polarizability can therefore be expressed using the Riemann zeta function $\zeta(x)$ as

$$\alpha_t = 3\sum_{n=0}^{\infty}\frac{(-1)^n}{(n+1)^3} = \frac{9}{4}\sum_{m=1}^{\infty}\frac{1}{m^3} = \frac{9}{4}\zeta(3) \approx 2.704\,63. \tag{13}$$
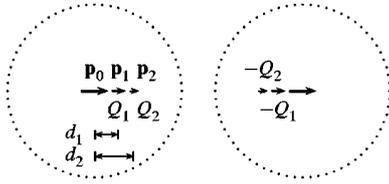
H. Wallen And A. Sihvola

FIG. 5. Image systems for the axial case.

B. Axial case

In the axial case the excitation $\mathbf{E}_0$ is parallel to the symmetry axis of the doublet, and the image system consists of both series of dipoles $\mathbf{p}_n$ and series of point charges Q_n.

Again, we first replace each sphere with a dipole $\mathbf{p}_0$ at the center of the sphere. Using Eq. (8) we get the images of the first dipoles at distance $d_1 = a^2/L$ from the center of the spheres as

$$p_1 = \frac{a^3}{L^3}p_0, \quad Q_1 = \frac{a}{L^2}p_0. \tag{14}$$

Then we need to compensate for both p_1 and Q_1, giving the images at distance $d_2 = a^2/(L-d_1)$ from the center of the spheres as

$$p_2 = \frac{a^3 p_1}{(L-d_1)^3}, \quad Q_2 = \frac{ap_1}{(L-d_1)^2} + \frac{aQ_1}{(L-d_1)}, \tag{15}$$

and so on as shown in Fig. 5. Note that all dipoles have the same direction as $\mathbf{E}_0$ and that the signs of the charges Q_1, Q_2 above are for the left sphere in the picture. All point charges in the right sphere have opposite signs.

Actually, we should also add a balancing charge $\mp Q_n$ at the center of the spheres at each step, but this would lead to an ever increasing number of series of point charges, which would be highly inefficient. Instead, we add an initial charge Q_0 at the center of the left sphere and $-Q_0$ at the center of the right sphere and require that the total charge in each sphere is zero. The recurrence equation for Q_n then becomes

$$Q_{n+1} = \frac{a}{L-d_n}Q_n + \frac{ap_n}{(L-d_n)^2}, \quad \sum_{n=0}^{\infty} Q_n = 0. \tag{16}$$

For d_n and p_n we get the same recurrence equations, Eqs. (9) and (10), as in the transversal case. This time all dipoles have the same orientation and furthermore we must take the charges into account when calculating the normalized polarizability as

$$\alpha_z = 3\sum_{n=0}^{\infty} \frac{p_n}{p_0} - 3\sum_{n=0}^{\infty} \left(\frac{L}{2} - d_n\right)\frac{Q_n}{p_0}. \tag{17}$$

Again, in the touching limit $L \to 2a$, we get the solutions in Eq. (12) for d_n and p_n and Eq. (16) is simplified to

$$Q_{n+1} = \frac{n+1}{n+2}Q_n + \frac{p_0}{a(n+1)(n+2)^2}. \tag{18}$$

This is a linear first-order difference equation of the form

$$x_{n+1} = c_n x_n + b_n, \tag{19}$$

which has the general solution[11]

$$x_n = \left(\prod_{k=0}^{n-1} c_k\right)x_0 + \sum_{m=0}^{n-2}\left(\prod_{k=m+1}^{n-1} c_k\right)b_m + b_{n-1}. \tag{20}$$

Using Eq. (20) and the summation formula

$$\sum_{k=1}^{n} \frac{1}{k(k+1)} = \sum_{k=1}^{n}\left(\frac{1}{k} - \frac{1}{k+1}\right) = 1 - \frac{1}{n+1}, \tag{21}$$

the solution of Eq. (18) can be simplified to

$$Q_n = \frac{(Q_0 + p_0/a)n + Q_0}{(n+1)^2}, \tag{22}$$

where Q_0 is yet to be determined. This presents a somewhat pathological problem since the sum $\Sigma_n Q_n$ diverges like the harmonic series unless we choose $Q_0 = -p_0/a$, but then again the total charge is still not zero:

$$\sum_{n=0}^{\infty} Q_n = \begin{cases} -\infty, & Q_0 < -p_0/a \\ -(p_0/a)\zeta(2), & Q_0 = -p_0/a \\ \infty, & Q_0 > -p_0/a. \end{cases} \tag{23}$$

The limiting value of the polarizability is, however, well defined if we set $Q_0 = -(p_0/a)(1+\delta)$ and let $\delta \to 0$, giving

$$\alpha_z = 6\zeta(3) - 3\delta\zeta(2) \xrightarrow{\delta \to 0} 6\zeta(3) \approx 7.212\,34, \tag{24}$$

in agreement with previously published results.[1–4]

V. SOLUTION OF THE RECURRENCE EQUATIONS

The recurrence equations for d_n, p_n, and Q_n can be solved also in the general case using some suitable substitutions and recurrence formulas for the Chebyshev polynomials.

Let us start with Eq. (9) for d_n. This is a special case of the Riccati equation,[11] whence we make a substitution

$$\frac{u_{n+1}}{u_n} = \frac{L-d_n}{a}, \quad u_0 = 1, \tag{25}$$

which gives an ordinary linear second-order recurrence equation

$$u_n = \frac{L}{a}u_{n-1} - u_{n-2}, \quad u_0 = 1, \quad u_1 = \frac{L}{a}. \tag{26}$$

Comparing the above with the recurrence relations for the Chebyshev polynomials[11]

$$T_{n+1}(x) = 2xT_n(x) - T_{n-1}(x), \quad T_0 = 1, \quad T_1 = x, \tag{27}$$

$$U_{n+1}(x) = 2xU_n(x) - U_{n-1}(x), \quad U_0 = 1, \quad U_1 = 2x, \tag{28}$$

we see that the general solution can be expressed as a linear combination of $T_n(L/2a)$ and $U_n(L/2a)$. Using the initial values we get $u_n = U_n(L/2a)$, whence the solution of Eq. (9) is

$$d_n = \frac{U_{n-1}(L/2a)}{U_n(L/2a)}a. \tag{29}$$

Now Eq. (10) for p_n can be easily solved as

$$p_n = \frac{a^3 p_{n-1}}{(L-d_{n-1})^3} = \frac{U_{n-1}^3 \cdots U_1^3 U_0^3}{U_n^3 U_{n-1}^3 \cdots U_1^3} p_0 = \frac{p_0}{U_n^3}, \tag{30}$$

where we have denoted $U_n = U_n(L/2a)$ for brevity. The normalized transversal polarizability can then be expressed as

$$\alpha_t = 3 \sum_{n=0}^{\infty} \frac{(-1)^n}{U_n^3}, \tag{31}$$

which is equivalent to the expression given by Levine and McQuarrie,[1] when we take into account the different normalizations used.

Using the solutions in Eqs. (29) and (30) for d_n and p_n, Eq. (16) for Q_n can be simplified to

$$Q_{n+1} = \frac{U_n}{U_{n+1}} Q_n + \frac{p_0}{a U_{n+1}^2 U_n}. \tag{32}$$

Using Eq. (20) we get the solution

$$Q_n = \frac{Q_0}{U_n} + \frac{p_0}{a U_n} \sum_{m=0}^{n-1} \frac{1}{U_{m+1} U_m}, \tag{33}$$

which simplifies to

$$Q_n = \frac{Q_0}{U_n} + \frac{U_{n-1}}{U_n^2} \frac{p_0}{a}, \tag{34}$$

using the formula

$$\frac{U_{n-1}}{U_n} = \sum_{k=0}^{n-1} \frac{1}{U_{k+1} U_k}, \quad n > 0, \tag{35}$$

which can be proven using induction after first deriving the auxiliary result $U_{n+1} U_{n-1} = U_n^2 - 1$. The authors were unable to find this summation formula in the literature, but it seems likely that we have just reinvented a not so well-known formula. The initial charge Q_0 is finally determined by the condition that the total charge is zero as

$$Q_0 = -\frac{p_0}{a} \left(\sum_{n=0}^{\infty} \frac{U_{n-1}}{U_n^2} \right) \left(\sum_{n=0}^{\infty} \frac{1}{U_n} \right)^{-1}. \tag{36}$$

To simplify the expression for the normalized axial polarizability, we first simplify

$$\frac{L}{2} - d_n = \frac{\frac{L}{2a} U_n - U_{n-1}}{U_n} a = \frac{(U_{n+1} - U_{n-1})}{2 U_n} a = \frac{T_{n+1}}{U_n} a, \tag{37}$$

using Eq. (28) and the formula[12] $U_{n+1} - U_{n-1} = 2 T_{n+1}$. Collecting the results, we have

$$\alpha_z = 3 \left(\sum_{n=0}^{\infty} \frac{1}{U_n^3} \right) - 3 \left(\sum_{n=0}^{\infty} \frac{T_{n+1} U_{n-1}}{U_n^3} \right)$$
$$+ 3 \left(\sum_{n=0}^{\infty} \frac{T_{n+1}}{U_n^2} \right) \left(\sum_{n=0}^{\infty} \frac{U_{n-1}}{U_n^2} \right) \left(\sum_{n=0}^{\infty} \frac{1}{U_n} \right)^{-1}, \tag{38}$$

which can be further simplified, using the formula[12] $T_n(x) = U_n(x) - x U_{n-1}(x)$, to

```
Require: L' ≥ 2, τ > 0
    α_t = p = 3
    d = 0
    while p < τ do
        p = -p/(L' - d)³
        d = 1/(L' - d)
        α_t = α_t + p
    end while
```

FIG. 6. Compute α_t as a function of $L' = L/a$. The final error is less than τ.

$$\alpha_z = 3 \left(\sum_{n=0}^{\infty} \frac{1}{U_n^3} \right) + \frac{6a}{L} \left(\sum_{n=0}^{\infty} \frac{T_n T_{n+1}}{U_n^3} \right)$$
$$- \frac{6a}{L} \left(\sum_{n=0}^{\infty} \frac{T_{n+1}}{U_n^2} \right) \left(\sum_{n=0}^{\infty} \frac{T_n}{U_n^2} \right) \left(\sum_{n=0}^{\infty} \frac{1}{U_n} \right)^{-1}. \tag{39}$$

All the series in Eq. (39) are convergent when $L > 2a$. The series converge rapidly when $L \gg 2a$, but near contact, $L \approx 2a$, the convergence is slow. In the limiting case, $L \to 2a$, we have $U_n \to n+1$, $T_n \to 1$, whence $\alpha_z \to 6\zeta(3)$ as before.

The equivalence between Eq. (39) and the expression given by Levine and McQuarrie[1] is not immediately obvious. The numerical results are, however, the same within the obtainable precision.

VI. NUMERICAL EVALUATION

A. Transversal case

In the transversal case, the alternating series in Eq. (11) can be evaluated by truncation. Figure 6 gives a straightforward implementation, which is quite efficient if $L > 2.01a$, or if only a modest precision is needed. For instance, for six digit precision, 100 terms are sufficient when $L = 2a$ and much fewer terms are needed when $L > 2a$.

Since the sum has alternating terms, the convergence can be dramatically improved using Euler's transformation[13]

$$\sum_{n=0}^{\infty} (-1)^n p_n = \sum_{n=0}^{k-1} (-1)^n p_n + \sum_{n=0}^{\infty} \frac{(-1)^n}{2^{n+1}} \Delta^n p_k, \tag{40}$$

where Δ is the forward difference operator,

$$\Delta^n p_k = \Delta^{n-1} p_{k+1} - \Delta^{n-1} p_k, \quad \Delta^0 p_k = p_k. \tag{41}$$

Using an implementation[14] of Euler's transformation, which optimizes the parameter k, we get 15 digits precision using no more than the 32 first terms. Furthermore, the terms are simple to compute iteratively using Eqs. (9) and (10).

Figure 7 shows the normalized transversal polarizability α_t as a function of $L/a = 0, \ldots, 5$. The values for the intersecting case $L/a < 2$ are computed using the formulas by Felderhof and Palaniappan.[5] Note that the polarizability is a continuous and smooth function for all $L/a > 0$.

B. Axial case

In the axial case, a brute force implementation of Eq. (17) is more complicated since the initial charge Q_0 is unknown. Figure 8 gives one reasonably simple implementation where the contribution from Q_0 is handled separately
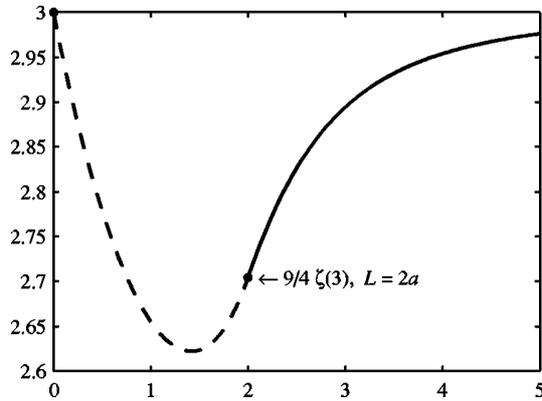
FIG. 7. Normalized transversal polarizability α_t as a function of L/a. The intersecting case (dashed line) is computed using the formulas by Felderhof and Palaniappan (see Ref. 5).
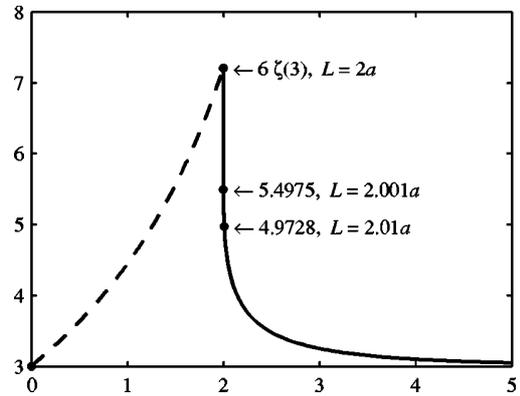

FIG. 9. Normalized axial polarizability α_z as a function of L/a. The intersecting case (dashed line) is computed using the formulas by Felderhof and Palaniappan (see Ref. 5).

(Q', etc.). The summation is stopped when the change is less than a given tolerance τ, but the actual precision achieved is worse. For $L > 2.01a$, the algorithm is reasonably fast and accurate, but for $L < 2.0001a$, we need many terms and start to lose precision.

The expression for the transversal polarizability, Eq. (31), is not very useful from a computational point of view, but in the axial case we can accelerate the convergence by converting the five series in Eq. (39) to alternating ones using the following van Vijngaarden transformation:[13]

$$\sum_{n=0}^{\infty} b_n = \sum_{k=0}^{\infty} (-1)^k a_k, \quad a_k = \sum_{j=0}^{\infty} 2^j b_{2^j(k+1)-1}. \quad (42)$$

Then, the new alternating series can be effectively computed using Euler's transformation. Using this approach, we can compute α_z for any $L > 2a$. This seems good enough for most practical purposes, but a further improvement would be to use a more sophisticated convergence acceleration technique such as the combined nonlinear-condensation transformation (CNCT).[15]

Figure 9 shows the normalized axial polarizability α_z as a function of $L/a = 0, \ldots, 5$. The values for the intersecting case $L/a < 2$ are computed using the formulas by Felderhof and Palaniappan.[5] The polarizability is a continuous function for all $L/a > 0$, but at contact $L/a = 2$ the right sided derivative is $-\infty$.

C. Asymptotics

For the axial case it would be interesting to know the asymptotic behavior of α_z as $L/a \to 2$. The first four series in Eq. (39) are approaching $\zeta(3)$ and $\zeta(2)$, but the series $\Sigma_n 1/U_n$ approaches the harmonic series and therefore diverges at contact.

Using a different approach Jeffrey and Onishi[16] found the asymptotics

$$\alpha_z \cong 6\zeta(3) - \frac{\pi^4}{6[\ln(2) + 2\gamma - \ln(\delta)]}, \quad \delta \to 0, \quad (43)$$

where $L/2a = 1 + \delta$. Numerically this seems to match our results, as seen in Fig. 10, but the connection to Eq. (39) seems hard to find.

VII. CONCLUSIONS

Using Kelvin's image principle, it is fairly simple to construct the series of images needed to calculate the transversal and the axial polarizability of a pair of conducting spheres. The series are, however, converging very slowly when $L \to 2a$.
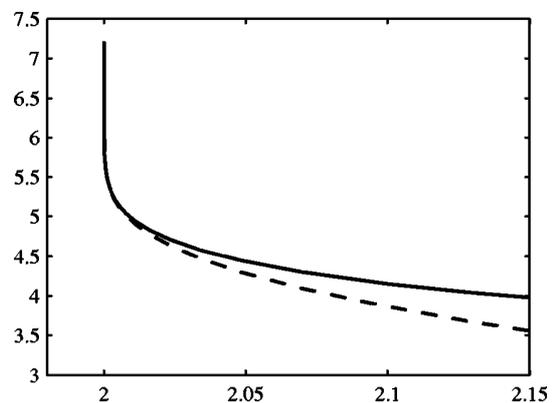

Require: $L' > 2, \tau > 0$
  $d = 0, \quad p = \alpha = \alpha_z = 3, \quad \alpha_z^{(-1)} = 0$
  $Q = \Sigma_Q = 0, \quad Q' = \Sigma_{Q'} = 1$
  $\alpha_{Q'} = L'/2$
  while $\alpha_z - \alpha_z^{(-1)} < \tau$ **do**
    $Q = p/(L' - d)^2 + Q/(L' - d)$
    $p = p/(L' - d)^3$
    $Q' = Q'/(L' - d)$
    $d = 1/(L' - d)$
    $\Sigma_Q = \Sigma_Q + Q, \quad \Sigma_{Q'} = \Sigma_{Q'} + Q'$
    $\alpha = \alpha + p - Q(L'/2 - d)$
    $\alpha_{Q'} = \alpha_{Q'} + Q'(L'/2 - d)$
    $\alpha_z^{(-1)} = \alpha_z, \quad \alpha_z = \alpha + \alpha_{Q'}\Sigma_Q/\Sigma_{Q'}$
  end while

FIG. 8. Compute α_z as a function of $L' = L/a$.

FIG. 10. Normalized axial polarizability α_z as a function of L/a. Asymptotics (see Ref. 16) (dashed line) compared to numerical results (solid line).

A very efficient way of calculating the transversal polarizability for any $L \geq 2a$ has been presented. But as was noticed in Sec. VI, the axial polarizability is much more difficult to calculate with high accuracy.

It is also instructive to connect the calculated polarizability results with physical principles. The polarizability is a measure of the object to become dipolarized. The normalized polarizability of a single sphere is $\alpha_s = 3$, and we can observe that for the transversal case we have $\alpha_t < \alpha_s$ and for the axial case we have $\alpha_z > \alpha_s$. The largest difference arises for touching spheres. This behavior is natural because for an elongated object (a prolate spheroid, for instance), the axial polarizability is larger and the transversal polarizability is smaller than for a sphere of the same size.[17] Note, however, that the trace of the polarizability (isotropic average) is always larger than that of a corresponding sphere.

The dramatical differences in the behavior near contact for the transversal and axial polarizability components can also be qualitatively explained using physical principles. In the transversal case, the two spheres are always at the same potential regardless of the distance L. Thus, one can expect that nothing dramatical happens when the spheres touch each other. In the axial case on the other hand, it is clear that there is a potential difference between the spheres when they are apart. At contact the potentials are forced to be the same, so we can expect some irregular behavior.

[1]H. B. Levine and D. A. McQuarrie, J. Chem. Phys. **49**, 4181 (1968).
[2]W. E. Smith and J. Rungis, J. Phys. E **8**, 379 (1975).
[3]T. B. Jones, J. Appl. Phys. **60**, 2226 (1986).
[4]J.C.-E. Sten and K. I. Nikoskinen, J. Electrost. **35**, 267 (1995).
[5]B. U. Felderhof and D. Palaniappan, J. Appl. Phys. **88**, 4947 (2000).
[6]J. D. Jackson, *Classical Electrodynamics*, 3rd ed. (Wiley, New York, 1999), Chap. 2.
[7]W. Thomson (Lord Kelvin), J. Math. Pures Appl. **10**, 364 (1845).
[8]W. Thomson (Lord Kelvin), *Reprint of Papers on Electrostatics and Magnetism* (Macmillan, London, 1872), Chaps. II and VI.
[9]J. C. Maxwell, *A Treatise on Electricity and Magnetism*, 3rd ed. (Clarendon Press, Oxford, 1891), Vol. 1, Chap. XI, art. 173, reprint (Dover, New York, 1954).
[10]W. R. Smythe, *Static and Dynamic Electricity*, 3rd ed. (Taylor & Francis, London, 1989), Chap. 5, revised printing.
[11]*CRC Standard Mathematical Tables and Formulae*, 30th ed., edited by D. Zwillinger (CRC, Boca Raton, 1996).
[12]*Handbook of Mathematical Functions*, edited by M. Abramowitz and I. A. Stegun (Dover, New York, 1972).
[13]*Modern Computing Methods*, 2nd ed. edited by C. W. Clenshaw, E. T. Goodwin, D. W. Martin, G. F. Miller, F. W. J. Olver, and J. H. Wilkinson (Philosophical Library, New York, 1961), Chap. 13.
[14]W. H. Press, B. P. Flannery, S. A. Teukolsky, and W. T. Vetterling, *Numerical Recipes in C: The Art of Scientific Computing*, 2nd ed. (Cambridge University Press, Cambridge, 1993).
[15]U. D. Jentschura, P. J. Mohr, G. Soff, and E. J. Weniger, Comput. Phys. Commun. **116**, 28 (1999).
[16]D. J. Jeffrey and Y. Onishi, J. Phys. A **13**, 2847 (1980).
[17]A. Sihvola, *Electromagnetic Mixing Formulas and Applications* (IEE, London, 1999), Chap. 4.